Grant Agreement No: 101096307

Full Title: THz Industrial Mesh Networks in Smart Sensing and Propagation Environments

Start date: 01/01/2023

End date: 31/12/2025

Duration: 36 Months

Deliverable D2.2

Definition of scenarios for software simulation

Document Type	Deliverable
Title	D2.2 - Definition of scenarios for software simulation
Contractual due date	31/08/2023 (M8)
Actual submission date	25/08/2023
Nature	Report
Dissemination Level	PUB
Lead Beneficiary	HWDU
Responsible Author	Tommaso Zugno (HWDU)
Contributions from	Lutfi Samara, Mate Boban (HWDU), Carla Reinhardt, Varvara Elesina, Steffen Pahlke (TUBS), Ahmed Shahhat (BI-REX), Carlo Lanzoni (AETNA), Giampaolo Cuozzo (CNIT)
Reviewers	Luca Sanguinetti (CNIT), Thomas Kürner (TUBS)

6GSNS

Revision history

Version	Issue Date	Changes	Contributor(s)
V0.0	05/06/2023	Document skeleton	Tommaso Zugno (HWDU)
V0.1	03/07/2023	Initial content	Tommaso Zugno (HWDU), Varvara Elesina, Carla Reinhardt (TUBS)
V0.2	04/08/2023	Inputs to Sec. 2, 3, 4, 5, 6.	Tommaso Zugno, Lutfi Samara (HWDU), Varvara Elesina, Carla Reinhardt, Steffen Pahlke (TUBS), Ahmed Shahhat (BI-REX), Carlo Lanzoni (AETNA), Giampaolo Cuozzo (CNIT)
V0.3	07/08/2023	Editorial modifications, inputs to Sec. 1 and 8, minor modifications to other sections.	Tommaso Zugno, Lutfi Samara, Mate Boban (HWDU), Varvara Elesina (TUBS)
V0.4	11/08/2023	Candidate Deliverable version	Tommaso Zugno (HWDU)
V0.5	22/08/2023	Addressed review comments	Tommaso Zugno (HWDU)
V1.0	25/08/2023	Final version	Tommaso Zugno (HWDU)

Table of Contents

List of Abbreviations

3GPP	3rd Generation Partnership Project
5G	5th Generation
6G	6th Generation
ACIA	Alliance for Connected Industries and Automation
AGVs	Automated Guided Vehicles
API	Application Programming Interface
AR	Augmented Reality
ASK	Amplitude-Shift Keying
AWGN	Additive White Gaussian Noise
BPSK	Binary Phase-Shift Keying
BM	Blockage Model
CAD	Computer-Aided Design
CDL	Clustered Delay Line
CIR	Channel Impulse Response
CSV	Comma Separated Values
DFT-S-OFDM	Direct Fourier Transform Spread OFDM
FDTD	Finite Difference Time Domain
FFT	Fast Fourier Transform
FMCW	Frequency Modulated Continuous Wave
FSK	Frequency Shift Keying
GAN	Generative Adversarial Network
GPU	Graphics Processing Unit
InF	Indoor Factory
ITU	International Telecommunication Union
KPI	Key Performance Indicator
LAN	Local Area Network
LL	Link-Level
LOS	Line-of-Sight
MAC	Medium Access Control
MIMO	Multiple Input Multiple Output
NLOS	Non-Line-of-Sight

NR	New Radio
OFDM	Orthogonal Frequency-Division Multiplexing
OOK	On–Off Keying
OCDM	Orthogonal Chirp Division Multiplexing
OPC UA	Open Platform Communications Unified Architecture
OTFS	Orthogonal Time Frequency Space modulation
PHY	Physical layer
PL	Path Loss
PLC	Programmable Logic Controller
PPM	Pulse Position Modulation
RMa	Rural Macrocell
RX	Receiver
RT	Ray Tracing
SBR	Shooting-Bouncing Ray
SC	Single Carrier
SC-FDE	Single-Carrier Frequency Domain Equalization
SINR	Signal to Interference plus Noise Ratio
SONs	Self Organizing Networks
STL	Standard Tessellation Language
TDL	Tapped Delay Line
THz	Terahertz
Uma	Urban Macro
Umi	Urban Micro
V2X	Vehicle-to-Everything

Executive Summary

The TIMES project aims at developing a THz-based smart radio ecosystem working in complex scenarios, with many heterogeneous devices capable of offering similar performance as wired networks. To achieve this goal, the project plans to design novel solutions at different layers of the protocol stack, build a new system architecture, and implement novel devices and RF components including front-ends, antennas, and intelligent reflecting surfaces. The approach that will be used for the assessment of the proposed solutions involves three main methodologies, i.e., theoretical analysis, software simulations, and hardware experiments. Software simulations will play a crucial role in the project, giving insights on the achievable performance without the need for real prototypes, and enabling the evaluation of use cases and scenarios that cannot be characterized through measurements yet. Different methodologies will be considered, including ray tracing for the characterization of THz wireless propagation, link-level simulations for the evaluation of physical layer solutions, and system-level simulations for the assessment of the overall system performance considering the presence of multiple nodes and the impact of data traffic and user mobility.

In this deliverable, we present models, parameters, and guidelines for conducting software simulations within the context of the TIMES project.

1. Introduction

Simulations are a widely used tool for the design and evaluation of wireless systems, as they allow to quantify performance without the need for real deployments or prototypes. They provide the possibility to examine the system under test in a controlled and reproducible environment and to assess its performance under different operating conditions. Different simulation methodologies are used in the field of wireless communications, the main ones being ray tracing, link-level, and system-level simulations. In general, these techniques make use of artificial models to account for external phenomena influencing the system behaviour. The accuracy of these models determines the level of realism that can be achieved through simulations, and therefore should be properly considered. For example, ray tracing simulations need an accurate representation of the propagation environment to characterize all propagation phenomena, while system-level simulations require detailed models for the mobility of wireless nodes and the behaviour of data traffic to obtain realistic results.

One of the tasks of this project is to define simulation scenarios and parameters to enable the accurate evaluation and establish a common baseline for the comparison of technological solutions developed by different partners. As part of this activity:

- We identified the most suitable simulation models for the modelling of industrial propagation environments, mobility of industrial robots, and data traffic generated by industrial applications;
- We defined a list of parameters for the modelling of wireless terminals based on the most recent literature, which will be updated at a later stage with findings obtained through measurements on real devices;
- We analyzed the use cases that have been identified in our previous deliverable (i.e., Deliverable D2.1) and specified the models and parameters for their simulation;
- We analyzed multiple simulation tools and identified the most suitable ones based on the project's needs.

The outcomes of this task are reported in this deliverable, which is meant to serve as a reference for project partners willing to conduct simulation campaigns. However, it does not preclude anyone from experimenting with other settings.

1.1 Scope

This deliverable presents simulation models, parameters, and guidelines for conducting software simulations, including ray tracing, link-, and system-level simulations. It compares different simulation tools and identifies the most suitable ones based on the project's needs.

1.2 Audience

This deliverable is mainly intended for participants of the TIMES project who need to conduct ray tracing, link- and/or system-level simulations.

1.3 Structure

The rest of the document is structured as follows:

- Section 2 presents the digital models of industrial environments to be used for the characterization of THz wireless channels through ray tracing simulations;
- Section 3 describes the mobility models for industrial robots that are needed for the evaluation of use cases with mobile terminals;

- Section 4 describes data traffic models mimicking the behaviour of the industrial applications targeted by the project;
- Section 5 lists the recommended parameters for the simulation of TIMES' wireless nodes;
- Section 6 provides guidelines on models and parameters to be used for the simulation of selected TIMES use cases;
- Section 7 presents an overview of simulation tools and their comparison;
- Section 8 concludes the deliverable.

2 Modeling of industrial propagation environments

In this project, we aim at characterizing the propagation of THz signals in industrial environments using both channel measurements and software simulations. One of the techniques that will be adopted is Ray Tracing (RT), a well-known and widely adopted approach which enables the accurate characterization of the channel behavior through simulations. RT simulations will be exploited to study environments where it is not possible to perform channel measurements. The resulting channel traces will be used to conduct channel modeling activities (as part of Work Package 3) and as an input for link- and system-level simulations (as part of Work Package 4). This will be essential to evaluate the communication and sensing performance of the solutions that will be developed throughout the project.

In the following, we review previous works on ray tracing simulations in industrial environments. Then, we present the virtual models of AETNA's RoboPac TechLab and BI-REX's pilot line that we developed as part of this task, and which are going to be used to conduct RT simulations throughout the project. These models are available to all the members of the consortium.

2.1 Literature review

The literature contains many studies exploiting RT simulations for the characterization of wireless channels. However, only a few deal with industrial environments at high frequencies. A summary of our analysis is presented in Table 1.

In [1], Niu et al. studied a realistic industrial environment with RT simulations and channel measurements at 6.75, 30, and 60 GHz. First, they scanned the industrial environment with a 3D laser scanner and transformed this data into a 3D CAD Model, which was then used to execute the simulation. Comparisons between the simulation results and the measurements showed that the strongest multipath components could be simulated, and significant scatterers could be identified.

In [2], Sheikh et al. studied the radio propagation of an Indoor Factory (InF) environment at 3.5, 28 and 60 GHz. For this purpose, a 3GPP-specified InF environment with dimensions 120 x 50 x 11 m was selected, characterized by a dense deployment of many obstacles. In the simulations, two distinct models were employed and subjected to comparison. The first is known as the blockage model, which exclusively allowed power reception under LOS conditions, while the second is a RT model. Two different network layouts with 6 and 12 base stations were considered. In each case, base stations were placed at the ceiling at a height of 11 m. The MATLAB RT tool was used to conduct simulation. The analysis showed that the blockage model provides unrealistic and pessimistic results for coverage/outage and too optimistic results in terms of SINR and throughput. The deterministic RT model is more realistic and suitable for an industrial indoor environment.

In [3], authors presented a novel platform for RT simulation that uses R-trees for 3D ray tracing path search considering two methods. The first is the image method, a point-to-point tracing algorithm that determines all rays passing through the receiver according to its position and all the reflection points. Because of its complexity, this approach is effective only in a simple environment. The second one is the shooting-bouncing ray method (SBR), where the transmitter emits rays in certain directions and track their propagation in space. The tracing is stopped when the strength of a ray is too low, or when the ray arrives at the receiver. The study considered an industrial space taken from [4] with dimensions 40.5 × 15.5 × 4.6 m. Both LOS and NLOS cases were considered, taking into account the dielectric parameters of the factory environment. The results show that path loss of LOS increases with frequency and distance. Path loss of NLOS also increases with distance.

However, due to obstacles it has local increasing and decreasing, that can be significantly different from LOS loss at the same distance.

The study presented in [5] included three steps. In the first step, RT simulation model was validated using of known realistic industrial environment and measurement results from article [4], considering 3.7 and 28 GHz frequencies. In the second step, the influence of different obstacles on electromagnetic wave propagation was analyzed by performing simulation with different clutter densities. In the last step, RT simulation to analyze different frequency bands at 2.6, 3.8, and 4.9 GHz was carried out considering an industrial space with dimensions of 50 × 50 × 9 m.

In [6] the authors present the Hybrid Method, a combination of RT and the Finite-Difference Time-Domain (FDTD) method, which directly solves Maxwell's equations in the time domain. RT works well in case of electrically large objects and perfectly conducting surfaces, meanwhile, the FDTD method better captures reflection, diffraction, and radiation effects while requiring high computation times. The proposed hybrid approach uses RT for wide and simple areas, while FDTD for areas that include complex obstacles and different dielectric properties. This hybrid method can be extremely effective for complex industrial environments.

Table 1 Summary of previous works about RT simulations in industrial environments

Reference	Environment	Frequency	Simulation tool	Useful points
[1]	Realistic industrial environment	6.75 GHz; 30 GHz; 60 GHz	Winprop	Space 3D laser scanning
[2]	3GPP specified InF environmental	3.5 GHz; 28 GHz; 60 GHz	Matlab (inhouse programmed RT-Tool)	Deterministic RT model is more suitable than Blockage Model
[3]	High-precision machining workshop hall	2.2 GHz; 3.7 GHz; 8.45 GHz	Tool developed by paper's authors	R-trees and combination of image and SBR RT methods; Dielectric properties should be considered
[5]	Realistic industrial environment, from [4]	3.7 GHz; 2.6 GHz; 3.8 GHz; 4.9 GHz	Not specified	Gradually increasing of clutter complexity in simulation scenario
[6]	Industrial indoor environment	3.5 GHz	REMCOM Wireless InSite; Sim4Life FDTD for FDTD	Hybrid Method, that combined RT and FDTD methods.

The main conclusion we can draw from the literature review above is that the research dedicated to the characterization of industrial environment at THz frequencies is very limited. However, from our analysis we can draw some useful considerations: (i) RT is a more suitable method for industrial environments compared to simplified methods such as the blockage model considered in [14]; (ii) the RT SBR method is preferable to the RT imaging method; (iii) when dealing with complex industrial spaces, it is necessary to consider the

dielectric properties of objects; (iv) a gradual increase of clutter complexity is a good approach for developing a comprehensive model; (v) the combination of RT and FDTD can be exploited to increase the accuracy.

2.2 Models of TIMES industrial environments

The characterization of wireless channels through RT simulations requires the detailed representation of the propagation environment, typically in the form of CAD models. As part of this task, we developed two models representing the industrial environments that are targeted by this project, namely BI-REX's pilot line and AETNA's RoboPac TechLab.

2.2.1 BI-REX Pilot Plant

The BI-REX pilot line is a prototyping space, which emulates a complete and integrated production plant. This space is used for testing and demonstrating new industrial technologies, as well as their integration with conventional systems. The area has a dimension of 22.04 × 14.24 m^2 and is divided into multiple thematic areas, including Big Data and Internet of Things, Additive Manufacturing, Robotics, finishing and metrology (Figure 1). Each thematic area includes one or multiple industrial machines, including a numerical control work center, three robotic arms, multiple AGVs, etc. A more detailed description is available in D2.1.

To characterize the channel behavior through ray tracing simulations, we created a virtual model of the pilot line using CAD software. The model includes the building layout, as well as industrial machines and other elements that are present in the environment and may impact the propagation of wireless signals. To account for the effect of materials, we separated the model into multiple parts, each including surfaces of the same material type. Each part was then exported in a separate STL file which can then be imported in the ray tracing tool and the corresponding material properties (i.e., relative permittivity and conductivity coefficients) can be applied. Figure 2 and Figure 3 show different views of the model.

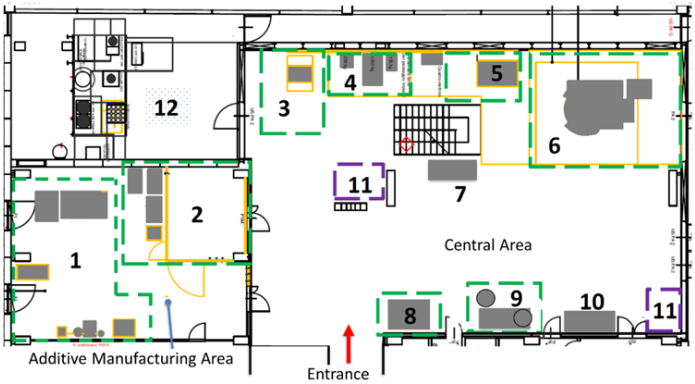

Figure 1 Layout of the BI-REX pilot plant

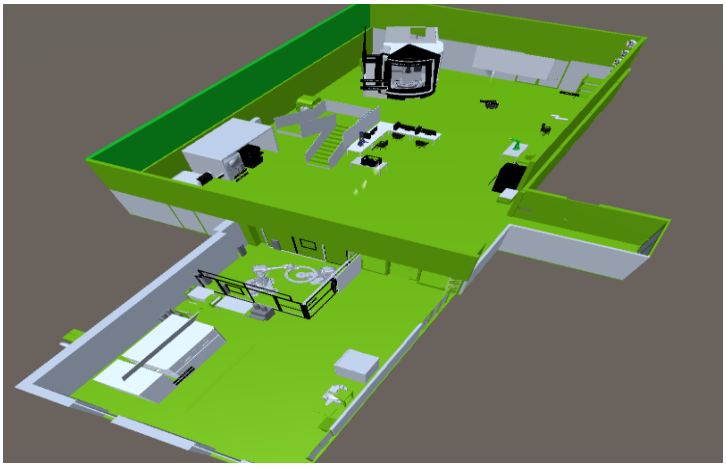

Figure 2 CAD model of the BIREX pilot plant (top view)

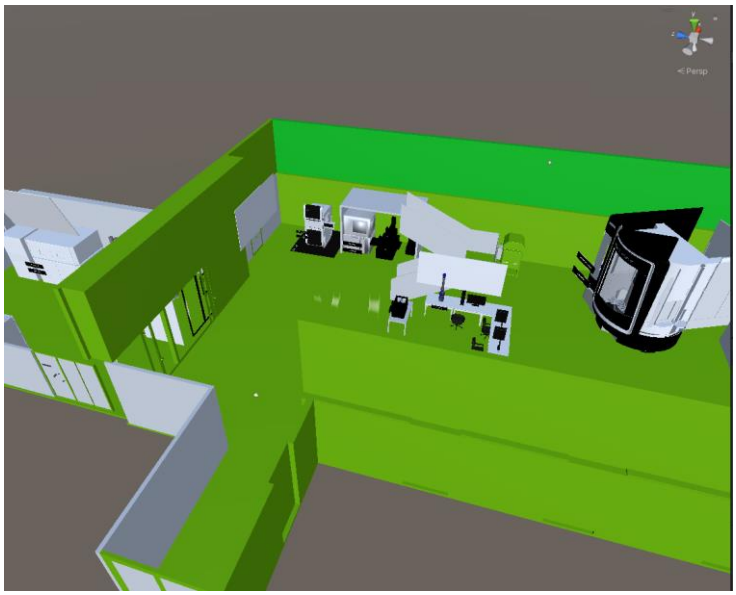

Figure 3 CAD model of the BIREX pilot plant (lateral view)

2.2.2 AETNA RoboPac TechLab

The RoboPac TechLab is a showroom dedicated to the demonstration and testing of industrial machines. The space covers an area of 400 m^2 and is located near Bologna (Italy) in one of the AETNA sites. Following the approach described in the previous section, we created a CAD model of TechLab which includes the building layout and three stretch-wrapper machines. Then, the model was separated into different parts depending on the material type and each part was exported in a separate STL file. With this approach, it will be possible to account for the electrical properties of materials when interacting with electro-magnetic waves. Figure 4 shows a view of the model, and Figure 5 shows a two-dimensional scheme representing the laboratory layout.

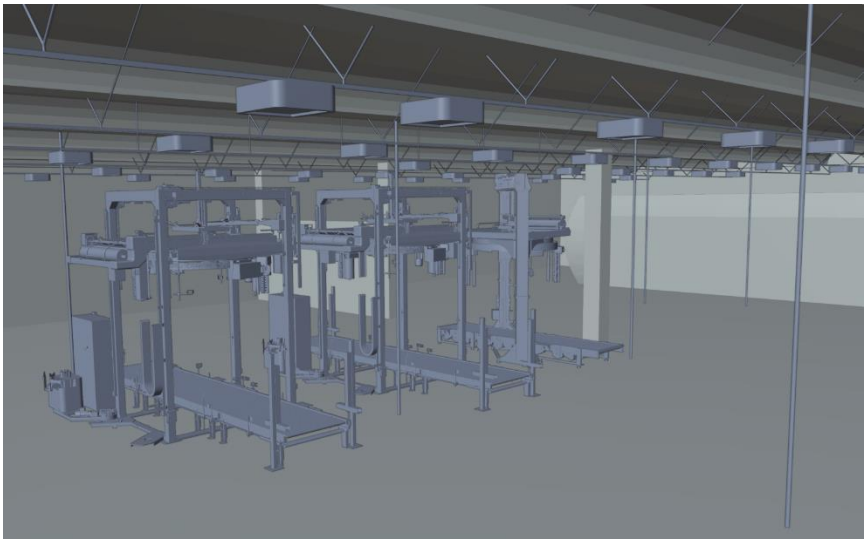

Figure 4 CAD model of AETNA's Robopac TechLab

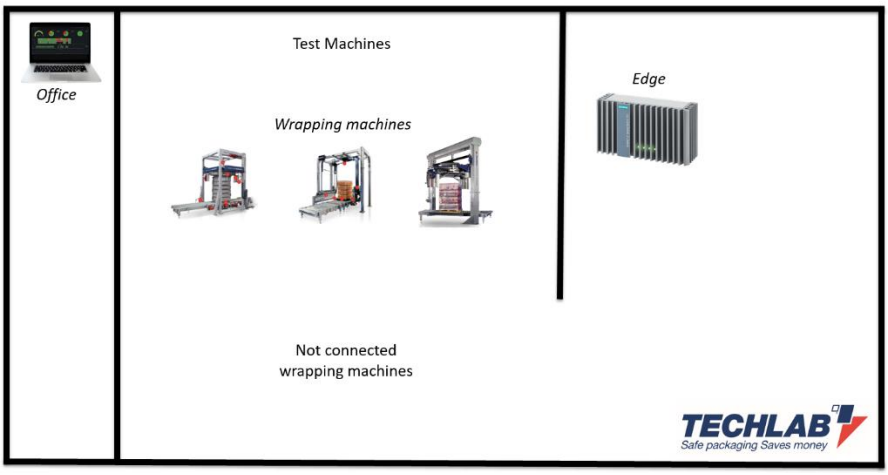

Figure 5 2D layout of AETNA's Robopac TechLab

3 Mobility models for industrial robots

Characterizing how wireless nodes and scatterers move through the environment is a fundamental aspect for the evaluation of mobile communication systems. Mobility induces variations in the wireless channel which, in turn, impacts communication performance. Typically, industrial use cases are characterized by harsh and dynamic propagation conditions, often happening in indoor environments with many moving nodes and scatterers. At the same time, they require extremely high reliability, thus making the characterization of mobility even more important.

The most common approach to simulate nodes' mobility consists in defining a stochastic model, which describes the evolution of nodes' positions over time. The main advantage of this approach is generalization, i.e., the possibility to abstract nodes' behavior as a random process and obtain multiple different realizations. However, it is difficult to define a model able to accurately represent real mobility patterns. Another approach is to consider real mobility traces collected through measurement campaigns. Compared to the first approach, this choice provides a higher level of realism but requires a considerable amount of effort for the data collection.

Several mobility models have already been proposed in the literature, especially for the evaluation of ad-hoc mobile networks [7] [8], and are available in system-level simulation platforms. One of the most popular is the random walk mobility model, where nodes move from their current location to a new location by randomly choosing direction and speed. Instead, with the random waypoint mobility model the node stays in one location for a certain period, then moves towards a new random destination at random speed. Finally, the Gauss-Markov mobility model updates the node's speed and direction at each time step following a correlation function. Despite their popularity, these models lack several features which limit the achievable level of realism. For example, they prevent the modeling of correlated mobility among different nodes and other behaviors that are commonly observed in real situations, such as avoiding obstacles or other nodes.

In recent years, more advanced models have been proposed. In [9], authors introduced a rule-based modular mobility model able to account for individual mobility, correlated mobility, collision avoidance, and enforcement of upper bounds. In [10], authors analyzed the behavior of automated guided vehicles in industrial environments and proposed a modified version of the random waypoint mobility model to better characterize the real mobility patterns.

3.1 Analysis of AGVs mobility patterns

Most of the models available in the literature represent mobile nodes as dimensionless points and characterize their linear motion, while orientation and angular velocities are typically ignored. However, when considering THz systems with highly directive antennas as in TIMES project, device orientation has a strong impact on signal propagation and should be carefully modeled for a proper system design. In [11] and [12], authors proposed an orientation-based random waypoint model that is suitable for user terminal devices. To better characterize this aspect in the context of mobile robots, we carried out an experiment with an AGV operating at BI-REX's premises and performing a standard mission. While the robot was operating, we acquired relevant mobility parameters, including position, orientation, linear and angular velocities. The data acquisition lasted for 50 seconds and the captured parameters were saved in a CSV file. In Figure 6, we represented the trajectory followed by the robot. Positions along x and y axis were measured by the robot itself and are relative to the position of the charging station. We can notice that the robot followed the same path multiple times. The maximum displacement along the x and y axis was 0.929 m and 11.084 m, respectively. Figure 7 represents the orientation of the robot during the acquisition period, while Figure 8 and Figure 9 show its linear and angular velocities.

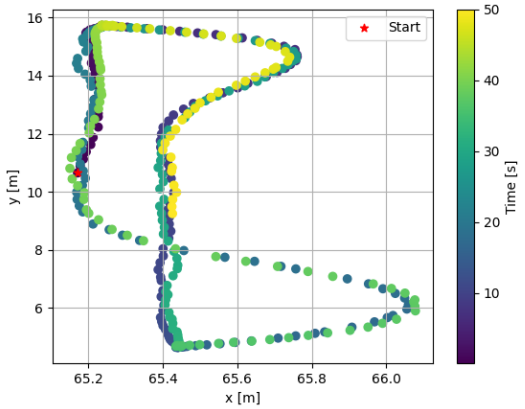

Figure 6 AGV trajectory

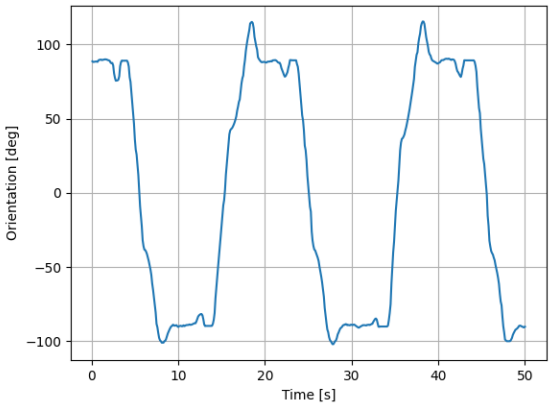

Figure 7 AGV orientation

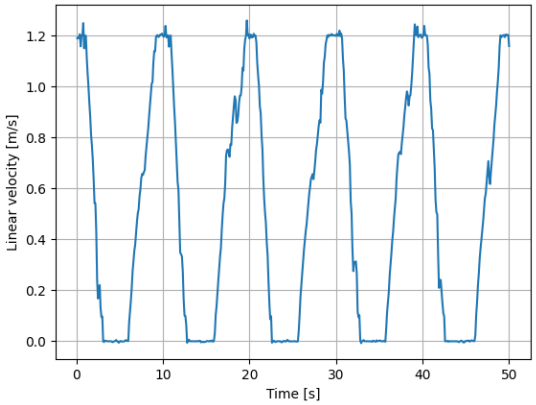

Figure 8 AGV linear velocity

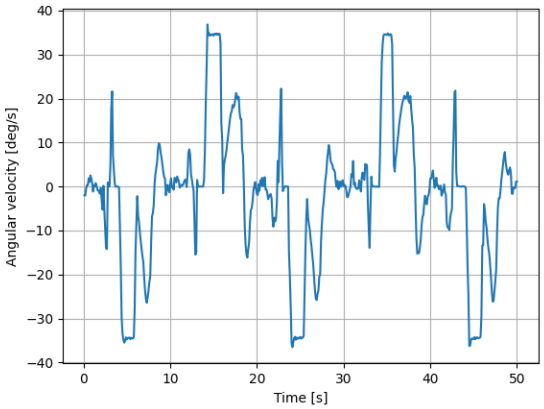

Figure 9 AGV angular velocity

From Figure 8, we can notice that the robot progressively increases and decreases its linear velocity until stopping and pausing for some time. During the pause time, linear movements are halted but the orientation may change, as shown in Figure 9. Following the approach in [11], we computed the coherence time for the angular motion as the time instant which satisfies $R_\alpha(0) = 0.05 * R_\alpha(T_{c,\alpha})$, where $R_\alpha(t)$ represents the autocorrelation function of the orientation angle.

Table 2 summarizes the results of our analysis. These values can be used as inputs for the extended orientation-based random waypoint model proposed in [12] to simulate AGVs in TIMES scenarios.

Table 2 AGVs mobility parameters

	Max	**Min**	**Avg**	**Std**
Absolute linear velocity [m/s]	1.260	0.000	0.525	0.473
Absolute angular velocity [deg/s]	36.845	0.000	11.034	11.950
Pause time for linear motion [s]	3.500	3.000	3.160	0.185
Coherence time for angular motion [s]	4.400			
x-axis displacement [m]	[65.150, 66.079]			
y-axis displacement [m]	[4.649, 15.733]			

4 Traffic models for industrial applications

The modelling of data traffic sources is another aspect to be considered for the simulation of wireless networks. This is particularly important when evaluating the performance of networking protocols, algorithms, and other solutions that are highly influenced by the traffic load. Data traffic models describe how traffic sources (e.g., applications) generate data to be transmitted though the network. Typically, data generation in a traffic source is modelled as a stochastic process with two main random variables, (i) time interval between two subsequent packets (i.e., inter-arrival time), and (ii) size of the generated data. The distribution of inter-arrival time and data size are obtained by collecting traffic traces and analysing the behaviour of real applications. In a simulation, each node in the network can host multiple sources with different characteristics, in such a way to emulate the presence of multiple logical links handled by different applications and generating different types of traffic.

Several traffic models are available in the literature. However, only a few are applicable to industrial use cases. Recently, the 5G Alliance for Connected Industries and Automation (5G-ACIA) published a report on traffic models for industrial use cases [13]. The report considers multiple use cases, including motion control, closed loop control, process monitoring, mobile robots, human-machine interface, closed-loop control, and control-to-control. For each use case, it specifies logical connections and data traffic models to be used in the simulation. In [14], the authors described three different traffic sources for industrial applications, including time-triggered traffic, audio-video bridging, and best effort. Moreover, they presented a novel ON/OFF-based model able to approximate the behaviour of the aforementioned sources. In [15], authors proposed a traffic model which makes use of a Generative Adversarial Network (GAN) to mimic realistic traffic sources. The GAN is trained with real traffic traces collected in different use cases, including industrial applications. However, in the case of industrial applications, the GAN-based model was used in conjunction with a stochastic-based model due to the lack of training data. In [16], authors proposed a two-step approach to model aggregated traffic sources in industrial networks, and validated the proposed method with real traffic traces.

Following the analysis provided in [17], we identified three main types of traffic that are of interest for the applications envisioned in TIMES. In the following, we describe each category and provide modeling guidelines.

4.1 Real-time traffic for motion control

This category includes the data traffic flows for the control of industrial processes. Typically, industrial machines are equipped with PLCs that send and receive information from I/O nodes to govern the industrial process. I/O nodes are located in different parts of the machine and connects multiple devices, e.g., sensors, servomotors, actuators, etc., that are collecting data values at every control cycle. The data flow between the PLC and each I/O node can be modelled as periodic traffic with constant inter-arrival time and fixed data size. The inter-arrival time depends on the type and duration of the control cycle of the industrial machine. As reported in [18], isochronous applications require a control cycle between 0.1 and 2 ms, while for non-isochronous applications the required cycle is typically between 2 to 20 ms. Instead, the data size depends on the type and quantity of data exchanged between I/O nodes and the PLC, which can vary between 30 and 100 bytes for simple sensors (e.g., temperature, humidity, etc.), and between 50 and 1500 bytes for high-end devices (e.g., cameras). Modelling parameters are reported in Table 3.

Table 3 Modelling parameters for real-time traffic for motion control

Parameter	Value		
Inter-arrival time (constant)	Isochronous applications:	0.1 - 2	ms
	Non-isochronous applications:	2 - 20	ms
Data size (constant)	Low-end sensors:	30 - 100	bytes
	High-end sensors:	50 - 1500	bytes

4.2 Traffic for vision systems

This category includes video traffic flows generated by cameras installed in industrial machines for the monitoring of manufacturing processes, or by AR headsets worn by industrial operators for a close interaction with machine and robots. Assuming that data compression is not applied, this traffic type can be modelled as a periodic flow with constant inter-arrival time and constant data size. The inter-arrival time depends on the frame rate of the camera, i.e., the frequency with which images are captured by the optical sensor. The frame rate for standard cameras is typically 30 Hz, while for slow-motion cameras it can increase up to 120 or 240 Hz. The data size depends on the video resolution, which defines the number of pixels in each frame, and the color depth, which corresponds to the number of bits used to encode each pixel. The resolution ranges from 720 x 1280 pixels for high-definition videos to 4320 x 7680 for full-ultra high-definition (also referred to as 8K) videos, while the color depth can vary from 24 to 48 bits. Like the analysis in [19], in Table 4 we reported the uncoded data sizes corresponding to different video resolutions and color depths.

Table 4 Uncoded data size in Mbytes for different frame sizes and color depths

	720 x 1280	1080 x 1920	1440 x 2560	2160 x 3840	2880 x 5120	4320 x 7680
24 bits	2.7648	6.2208	11.0592	24.8832	44.2368	99.5328
36 bits	4.1472	9.3312	16.5888	37.3248	66.3552	149.2992
48 bits	5.5296	12.4416	22.1184	49.7664	88.4736	199.0656

Depending on the combination of resolution and color depth, we can identify three different device categories: low end (in yellow), medium end (in blue), and high end (in green). Based on the above considerations, in Table 5 we list the proposed modelling parameters.

Table 5 Modelling parameters for vision systems

Parameter	Value		
Inter-arrival time (constant)	Standard camera:	1/30	s
	Slow motion camera:	1/120	s
Data size (constant)	Low end camera:	2 - 12	Mbytes
	Medium end camera:	12 - 45	Mbytes
	High end camera:	45 - 200	Mbytes

4.3 Non-real-time traffic for data collection and optimization

This category includes traffic flows used to collect measurement data from the industrial machines and exchange information for the optimization of the industrial process. In this case, to better understand the traffic generated in TIMES use cases, we performed a data traffic acquisition on a real industrial process running in AETNA's Robopac TechLab. We considered a packaging process where a small wrapping machine is automatically stretching a plastic film around a pallet to stabilize the load for its transport. The machine is equipped with a PLC and multiple sensors. The PLC is connected to an edge computer and shares measurement data captured from the sensors. The edge computer is processing the received data and is sending messages to the PLC containing manufacturing recipes, i.e., sets of parameters to adjust the machine configuration. In this setting, we analyzed the data traffic exchanged between the PLC and the edge computer by performing a packet capture with Wireshark [20]. The data acquisition lasted for 97.35 seconds, and the capture log was saved in the PCAP format. We analyzed the capture log and identified the different traffic flows by grouping packets based on the direction of communication, i.e., either UL (from the PLC to the edge computer) or DL (from the edge computer to the PLC), and the application protocol used for the information exchange. Four different flows can be identified. The first (UL OPC UA) and the second (DL OPC UA) flows are used to exchange manufacturing recipes and diagnostic information between the edge computer to the PLC and acknowledge their reception. These flows make use of the OPC UA protocol, which enables the asynchronous message exchange between the two nodes. The third (UL Modbus TCP) and the fourth (DL Modbus TCP) flows are used to upstream the measurement data from the PLC to the edge computer and to acknowledge their reception. These flows make use of the Modbus TCP protocol which enables a synchronous message exchange between the two nodes. In Figure 10, we represented the packet length over time for the different flows.

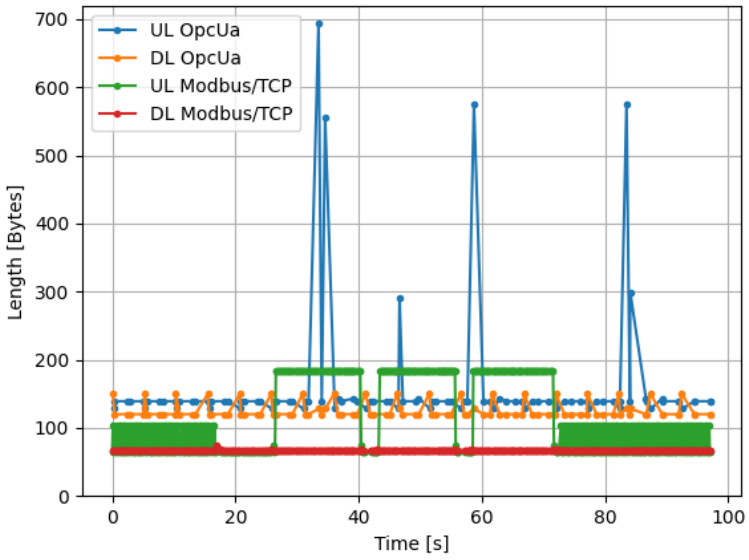

Figure 10 Packet length vs time for different traffic flows

As shown in the figure, traffic is higher in the UL direction, as the PLC is upstreaming measurement data and diagnostic information which are heavier than configuration messages sent in the DL direction.

4.3.1 Traffic flow for data collection

In the UL direction, the Modbus TCP flow shows a burst starting at 26.57 s and ending at 71.57 s, with a duration of 45 s. In this period, the industrial machine was operating and performing wrapping operations, while before and after the burst the machine was in standby mode, waiting for the pallet to be loaded or unloaded. When the machine is in standby mode, the packet size is between 65 and 103 bytes, with a weighted average of about 75 bytes. The size increases up 183 bytes when in operation. In the DL direction, the Modbus TCP traffic shows a periodic behavior with an almost constant packet size of 66 bytes. The inter-arrival time statistics are similar for both DL and UL flow and exhibit the same behavior during the entire acquisition period, irrespective of the machine status. Both inter-arrival time and data size statistics are summarized in Table 6.

Table 6 Statistics of Modbus TCP flows observed in real traces

	Inter-arrival time [s]				Data size [bytes]			
Direction	**Max**	**Min**	**Avg**	**Std dev**	**Max**	**Min**	**Avg**	**Std dev**
UL	1.110	0.069	0.134	0.066	183	65	119.607	54.845
DL	1.140	0.022	0.134	0.072	75	66	66.068	0.549

Following the observations above, traffic in the UL direction can be modelled as a two-state stochastic process characterized by two alternating states corresponding to the operation modes of the industrial machine, namely *standby* and *ON*. In each state, the traffic source generates packets with constant size and inter-arrival time for a period. The duration of the *standby* state ($T_{standby}$) represents the time needed to load and unload the machine and prepare it for a new cycle. Since this operation is typically carried out by human operators, we assume $T_{standby}$ to be a random variable with exponential distribution (indicated with the symbol $Exp\ (\lambda)$, where $\frac{1}{\lambda}$ corresponds to its mean). Furthermore, we assume the duration of the *ON* state (T_{ON}) to be fixed, as it represents the time it takes for the machine to complete a manufacturing cycle. Moreover, we assume the same inter-arrival time for both states while the packet size to be higher during the ON period, as observed in our measurements. Traffic in the DL direction can be modeled as a periodic source with constant inter-arrival time and data size. Figure 11 and Figure 12 illustrate the proposed models, while Table 7 provides the suggested model parameters.

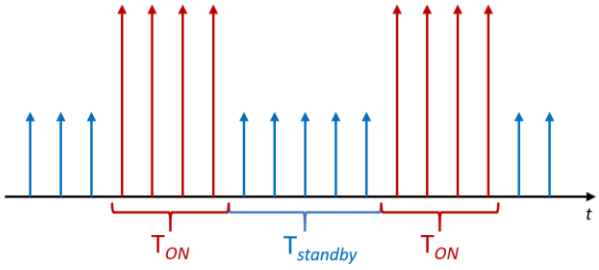

Figure 11 Model for UL Modbus/TCP traffic

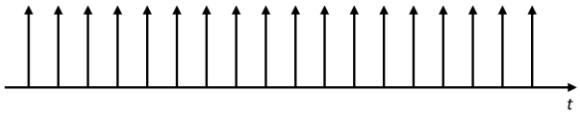

Figure 12 Model for DL Modbus/TCP traffic

Table 7 Modelling parameters for data collection traffic flows

	Parameter	Value	
UL	Inter-arrival time (constant)	1 - 100	ms
	Data size ON (constant)	100 - 1500	bytes
	Data size STANDBY (constant)	30 - 100	bytes
	T_{ON} (constant)	10 - 60	s
	$T_{standby}$ (random)	$Exp\ (\lambda), \frac{1}{\lambda} \in [30, 120]$	s
DL	Inter-arrival time (constant)	1 - 100	ms
	Data size (constant)	30 - 100	bytes

4.3.2 Traffic flow for machine optimization

As shown in Figure 10, the OPC UA flows exhibit an aperiodic behaviour with asynchronous messages exchanged between PLC and edge computer. Also, in this case we can observe some burst in the UL direction, however, they are not limited to the time period where the machine is operating. Instead, the DL traffic presents a more stable behaviour. Data size and inter-arrival time statistics for both UL and DL flows are summarized in Table 8.

Table 8 Statistics of OPC UA flows observed in real traces

	Inter-arrival time [s]				Data size [bytes]			
Direction	**Max**	**Min**	**Avg**	**Std dev**	**Max**	**Min**	**Avg**	**Std dev**
UL	2.584	0.035	1.002	0.729	694	128	159.299	94.819
DL	2.588	0.010	1.002	0.721	150	120	126.371	11.818

For a simplified modelling of the observed traffic flows, we assume packets to be generated with exponentially distributed IPI in both directions. We consider the packet size to be constant in the DL direction, and to behave as a binary random variable in the UL direction able to assume either a high or a low value. The probability of assuming the high value (P_{high}) is proportional to the frequency of traffic bursts. Modelling parameters are reported in

Table 9.

Table 9 Modelling parameters for machine optimization traffic flows

	Parameter	Value	
UL	Inter-arrival time (random)	$Exp\ (\lambda), \frac{1}{\lambda} \in [0.01,\ 1]$	s
	Data size high (constant)	500 - 1500	bytes
	Data size low (constant)	100 - 300	bytes
	P_{high}	0.05 - 0.1	
DL	Inter-arrival time (random)	$Exp\ (\lambda), \frac{1}{\lambda} \in [0.01,\ 1]$	s
	Data size (constant)	100 - 300	bytes

5 Models and parameters for wireless nodes

Table 10 provides examples of simulation parameters for the modeling of wireless nodes. The parameters are divided into two categories that correspond to certain capabilities of a transceiver device. Two types of devices are identified: a low-end device, suitable for user terminals, sensors, small robots, etc., and high-end devices, emulating e.g., an access point communicating with a machine or a generic device in the industrial environment, or inter-machine communications.

Table 10 Recommended simulation parameters for wireless nodes

Symbol	Parameter	Device Type	
		Low-end	**High-end**
P_T	Transmit power	-10 to 0 dBm [21] [22]	Up to 25 dBm [23]
NF	Noise Figure	10-15 dB [24]	8 dB [23]
$G_{Tx/Rx}$	Antenna gains	6 dBi [23]	Up to 55 dBi [25]
-	Frequency range	0.2 to 1.5 THz	
B	Bandwidth	Starting from 0.5 GHz [26], up to 2.16 GHz [23]	Up to 100 GHz [26]
-	Modulation type	OOK [23], PPM [27], BPSK [23]	8-PSK, *M*-QAM | *M*=4,16,64 [23]
N	FFT size	64, 128	{256 [28], 512, 1024, 2048, 3168 [29], 4096 [30]}
N_{TC}	No. of transceiver chains	Up to 256	
N_A	Antenna array size	{1,2,4,6,20} [31]	16 by 16 [32]
τ_s	Beam-switching time	10 ns	

The above parameters are given with the intention of providing guidance to project members that will perform simulation studies and are by no means meant to be restrictive. For instance, the antenna array size of 16 by 16 can be increased when simulating an ultra-massive MIMO setup. Larger array sizes are envisioned to be deployed in the THz band, as discussed in e.g., [33] and the references therein, but to the best of our knowledge, no hardware demonstration has been reported at the THz bands with such large antenna array sizes due to the complexity of realizing such systems.

Modulation orders have been mainly borrowed from the IEEE 202.15.3d-2017 standard [23]. We suggest to consider low-complexity waveforms (such as OOK, PPM, OFDM with small FFT size) for low-end devices, and waveforms with higher complexity (such as OFDM [30] [33], DFT-s-OFDM [30], SC-FDE [30], AFDM w/o OTFS [28], and OCDM [34]) for high-end devices. Further considerations will be made by Task 4.2, which will design new waveforms for integrated sensing and communications scenarios. For instance, the DFT-S-OFDM waveform is currently being considered as an option to help reduce PAPR.

Table 11 provides recommended noise models that should be considered when operating at THz frequencies, including molecular and local oscillator phase noise. The latter is particularly important as it represents a limiting factor for the efficiency of THz devices [34]. The Wiener-Gaussian model is more suitable for analytical studies, while the 3GPP model is a more practical alternative using a power spectral density-based approach. While the loop bandwidth is mapped to the device type, where a lower loop bandwidth is assigned to the phase noise model of the higher end device, no specific numbers are given at this stage, and an update of the phase noise model will be provided as an outcome of Task 4.1 in Work Package 4.

Table 11 Recommended models for hardware impairments

Model		**Device Type**	
		Low-end	**High-end**
Molecular noise model		Based on [35]	
Phase noise model			
	Wiener-Gaussian [34], Reference oscillator [35]	Ratio of correlated to uncorrelated phase: low	Ratio of correlated to uncorrelated phase: high
	3GPP [36]	Loop BW: High	Loop BW: Low

6 Simulation scenarios for TIMES use cases

In the following, we present a list of simulation scenarios that are based on a selected subset of TIMES use cases defined in [17]. These scenarios can be used to carry out software simulations with the goal of assessing the performance of technological solutions developed throughout the project. For each scenario, we detail:

- the related use case described in [17];
- the industrial environment where the use case is executed, either the BI-REX pilot plant or AETNA's Robopac Techlab presented in Section 2.2;
- the type and number of nodes involved, including the corresponding device category to be used for the selection of the simulation parameters presented in Section 5;
- the communication links to be established and their direction;
- the service flows describing the sequence of actions and events happening during the use case execution;
- the data traffic models to be used for the modeling of data generation which refer to those presented in Section 4;
- when applicable, the mobility models to be used for the modeling of nodes' mobility which refer to those presented in Section 3.

6.1 Scenario 1: Automated and guided vehicles and robots

Use Case	Automated and guided vehicles and robots
Environment	BI-REX's pilot line
Nodes	• 1 – 5 edge computers (high-end devices) • 1 – 10 AGVs (low-end devices)
Communication links	• Edge computers <-> AGVs
Service flows	• AGVs upstream sensor data to edge computers • Edge computers deliver control commands to AGVs
Data traffic models	• Real-time traffic for motion control (Section 4.1) between edge computers and AGVs
Mobility models	• AGVs mobility model (Section 3.1)

6.2 Scenario 2: Online cooperative high-resolution 3D map building

Use Case	Online cooperative high-resolution 3D map building
Environment	BI-REX's pilot line
Nodes	• 1 – 5 edge computers (high-end devices) • 1 – 10 AGVs (low-end devices)
Communication links	• Edge computers <-> AGVs • AGVs <-> AGVs
Service flows	• AGVs upstream sensor data to edge computers • Edge computers deliver control commands to AGVs • AGVs share sensor data among themselves

Data traffic models	• Real-time traffic for motion control (Section 4.1) between edge computers and AGVs • Non-real time traffic for data collection among AGVs (Section 4.3.1)
Mobility models	• AGVs mobility model (Section 3.1)

6.3 Scenario 3: Predictive Maintenance

Use Case	Predictive Maintenance
Environment	AETNA
Nodes	• 1 – 10 edge computers (high-end devices) Low/medium complexity machines: • 15 – 20 I/O nodes (low-end devices) • 1 – 5 PLCs (low-end devices) High complexity machines: • 20 - 100 I/O nodes (low-end devices) • 10 – 100 PLCs (low-end devices)
Communication links	• I/O nodes -> PLCs • PLCs <-> edge computers
Service flows	• I/O nodes upstream data to PLCs • PLCs forward collected data to the edge computers • Edge computers deliver configuration messages to PLCs
Data traffic models	• Real time traffic for motion control (Section 4.1) between I/O nodes and PLCs • Non-real time traffic for data collection (Section 4.3.1) between PLCs and edge computers • Non-real time traffic for machine optimization (Section 4.3.2) between PLCs and edge computers

6.4 Scenario 4: Fast process monitoring with a mix of mechatronic data and video, high feature remote access and maintenance

Use Case	Fast process monitoring with a mix of mechatronic data and video, high feature remote access and maintenance
Environment	AETNA's RoboPac TechLab
Nodes	• 1 – 10 edge computers (high-end devices) Low/medium complexity machines: • 15 – 20 I/O nodes (low-end devices) • 1 – 5 PLCs (low-end devices) • 1 – 10 cameras (low-end devices) High complexity machines: • 20 - 100 I/O nodes (low-end devices) • 10 – 100 PLCs (low-end devices)

	• 10 – 100 cameras (low-end devices)
Communication links	• I/O nodes -> PLCs • PLCs <-> edge computers • Cameras -> edge computers
Service flows	• I/O nodes upstream data to PLCs • PLCs forward collected data to the edge computers • Cameras stream video to edge computers • Edge computers deliver configuration messages to PLCs
Data traffic models	• Real time traffic for motion control (Section 4.1) between I/O nodes and PLCs • Non-real time traffic for data collection (Section 4.3.1) between PLCs and edge computers • Non-real time traffic for machine optimization (Section 4.3.2) between PLCs and edge computers • Video streaming traffic (Section 4.2) between cameras and edge computers

6.5 Scenario 5: Ultimate immersive cloud VR/AR

Use Case	Ultimate immersive cloud VR/AR
Environment	BI-REX's pilot line
Nodes	• 1 – 10 human operators equipped with AR devices (low-end devices) • 1 - 5 PLC (low-end devices) • 1 edge computer (high-end devices)
Communication links	• AR devices <-> edge computer • PLCs <-> edge computers
Service flows	• PLCs sends status information to edge computer • Edge computer receives camera images captured by AR device, generates virtual images displaying machines status, and transmits them to the AR devices
Data traffic models	• Non-real time traffic for data collection (Section 4.3.1) between PLCs and edge computers • Video streaming traffic (Section 4.2) between AR devices and edge computer
Mobility models	• Random-walk mobility model for human operators

6.6 Scenario 6: Motion controller – virtual PLC

Use Case	Motion controller – virtual PLC
Environment	AETNA's RoboPac TechLab
Nodes	• 1 – 5 edge computers (high-end devices) Low/medium complexity machines: • 15 – 20 I/O nodes (low-end devices)

	High complexity machines: • 20 - 100 I/O nodes (low-end devices)
Communication links	I/O nodes <-> edge computers
Service flows	• Virtual PLC collects data from sensors • Virtual PLC processes the collected data and sends commands to actuators
Data traffic models	Real time traffic for motion control (Section 4.1) between I/O nodes and edge computers

6.7 Scenario 7: Control-to-control communication (motion subsystems)

Use Case	Control-to-control communication (motion subsystems)
Environment	AETNA's RoboPac TechLab
Nodes	Low/medium complexity machines: • 15 – 20 I/O nodes (low-end devices) • 1 – 5 PLCs (low-end devices) High complexity machines: • 20 - 100 I/O nodes (low-end devices) • 10 – 100 PLCs (low-end devices)
Communication links	• I/O nodes <-> PLCs • PLCs <-> PLCs
Service flows	• PLCs collect data from sensors • PLC processes the collected data and PLCs send commands to actuators • PLCs exchange information to synchronize their operations
Data traffic models	• Real time traffic for motion control (Section 4.1) between I/O nodes and PLCs • Real time traffic for motion control (Section 4.1) among PLCs

6.8 Scenario 8: Mobile control panels with safety functions

Use Case	Mobile control panels with safety functions
Environment	AETNA's RoboPac TechLab
Nodes	Low/medium complexity machines: • 1 – 5 PLCs (low-end devices) High complexity machines: • 10 – 100 PLCs (low-end devices)
Communication links	• Mobile control panels <-> PLCs
Service flows	• PLCs transmit status information to mobile control panels • Mobile control panels transmit control messages to configure machine operations

Data traffic models	• Non-real time traffic for data collection (Section 4.3.1) between PLCs and mobile control panels • Non-real time traffic for machine optimization (Section 4.3.2) between mobile control panels and PLCs
Mobility models	• Random walk mobility model for mobile control panels

6.9 Scenario 9: Real-time cooperative safety protection

Use Case	Real-time cooperative safety protection
Environment	BI-REX's pilot line
Nodes	• 1 – 10 human operators • 2 – 20 AGVs (low-end devices)
Communication links	• AGVs <-> AGVs
Service flows	• AGVs exchange collected data and avoid potential risks for human operators
Data traffic models	• Non-real time traffic for data collection among AGVs (Section 4.3.1)
Mobility models	• AGVs mobility model (Section 3.1) • Random walk mobility model for human operators

6.10 Scenario 10: Collaborative robots in groups

Use Case	Collaborative robots in groups
Environment	BI-REX's pilot line
Nodes	• 2 – 20 AGVs (low-end devices) • 1 – 5 edge computers (high-end devices)
Communication links	• AGVs <-> AGVs
Service flows	• AGVs exchange data among themselves • AGVs upload sensing data to the edge computers • Edge computers issue control commands to AGVs
Data traffic models	• Non-real time traffic for data collection among AGVs (Section 4.3.1) • Non-real time traffic for data collection (Section 4.3.1) between AGVs and edge computers • Non-real time traffic for machine optimization (Section 4.3.2) between edge computers and AGVs
Mobility models	• AGVs mobility model (Section 3.1)

7 Simulation tools

In this section, we provide an overview of simulation tools that can be used to evaluate the performance of technological solutions that will be developed throughout the project. We considered three main categories, i.e., ray tracing, link-level, and system-level simulation tools.

7.1 Overview of ray tracing tools

To identify the best RT tool that fits our needs, we analyzed four different options and highlighted the main features and limitations. In the following, we describe the selected tools, while in Table 12 we summarize their main features.

SiMoNe ray tracing simulator

Simulator for Mobile Networks (SiMoNe) is a simulation framework that includes a system-level simulator, a link-level simulator and a propagation simulation tool. It was developed at the Institute of Communication Technology at TU Braunschweig for the analysis of mobile communication systems in realistic scenarios and environments [37] [38]. There are several different approaches to propagation simulation in SiMoNe:

1) a tool employing empirical models such as Okumura Hata mainly for outdoor macrocells;

2) an analytical 3D ray-launcher for indoor and outdoor cells;

3) a 3D indoor-outdoor ray-tracer, considering full 3D building information for cells that are usually indoors, with supporting hierarchical structures (like doors or windows) [37].

SiMoNe enables comprehensive multipath simulations including all interesting effects such as reflection, scattering and diffraction and material properties libraries based on information from different sources such as measurement results, e.g., [39] and ITU-R P2040-2 [40]. It is possible to extend the material properties list and this work is ongoing. There is the possibility for quasi-static simulation, the addition of time-variant simulation options is in development. Also, SiMoNe has already been successfully used for propagation simulations with a carrier frequency of 300 GHz [41].

Opal

Opal is a radio-frequency propagation simulator which is part of the open-source Veneris framework [42]. It makes use of the SBR method to simulate wireless propagation and supports both static and moving 3D scene objects represented as triangle meshes. It is implemented in C++ and utilizes NVIDIA OptiX, a GPU-based RT engine. Opal provides different RT options: it is possible to create rays "manually" or automatically generate rays based on built-in models. Material properties are accounted according to the ITU-R P.2040 recommendation [43], which supports a frequency range from 1 GHz to 100 GHz. The highest frequency that was simulated in research with Opal is 5.9 GHz [44].

Altair WinProp

Altar WinProp is a commercial tool for signal propagation modeling and network planning. WinProp is available for a wide range of scenarios, from basic indoor to dynamic and satellites scenarios [45]. WinProp was successfully used for the characterization of industrial environments at 6.75, 30 and 60 GHz [1]. However, the frequency range is limited to 100 GHz, as it is based on the ITU-R P.1411 recommendations [46] for the modeling of material properties.

Sionna ray tracing simulator

Sionna is an open-source library developed and maintained by NVIDIA, which also provides detailed documentation [47] and quick-response customer service in case of questions. Sionna is based on TensorFlow and is programmed in a block structure in which almost all blocks are differentiable. Following this, it is possible to replace a block with a trainable neural network to integrate machine learning algorithms into the signal processing chain. It is also possible to use a GPU to accelerate computation time [48]. Since the release of v0.14.0 a ray tracer has been integrated in Sionna. The scene in which the ray tracing is performed is created in Blender and exported with the Mitsuba-Blender add-on. It is also possible to import a scene from OpenStreetMaps into Blender with the Blender-OSM add-on. It is possible to visualize the scene and the paths found by the ray tracing by rendering. Since only the radio material properties which are defined by ITU-R P.2040-2 are implemented [40], most of the radio material properties are not defined for frequencies above 100 GHz. Only glass and ceiling board properties are defined for frequency band 220 – 450 GHz. However, it is possible to define custom materials to implement the radio material properties for carrier frequencies around 300 GHz [49].

Table 12 Comparison of RT simulation tools

Tool	Open source	Frequency band	Scenario	Time variant	Material properties
SiMoNe	No	Up to 300 GHz	Indoor office, urban outdoor micro and macrocell, V2X	Quasi-static	Built-in libraries, based on different sources: measurements [39], ITU recommendation ITU-R P.2040-2 [46], etc. It is possible to add new materials
Opal (part of Veneris)	Yes	Up to 100 GHz	Vehicular scenarios in urban outdoor environment	Yes	Recommendation ITU-R P.2040 (Up to 100 GHz) [43]
Altair WinProp	No	Up to 100 GHz	Rural; urban and sub-urban; indoor and campus; tunnel and underground; vehicular and time-variant; GEO, LEO satellites	Yes	Recommendation ITU-R P.2040-1 (Up to 100 GHz) [50]
Sionna	Yes	Up to 100 GHz **Possible extension up to 300 GHz**	rural macrocell; urban outdoor micro and macrocell	No	Recommendation ITU-R P.2040-2 Most part of materials defined up to 100 GHz, two materials up to 450 GHz [40]

There are currently a wide range of ray tracing tools available, each with its own advantages and disadvantages, depending on the application area and goals. In the review presented above, four ray tracing tools are compared (Table 12). Based on this comparison, we can conclude that WinProp and Opal do not fit

project's need, as WinProp is not publicly available, and Opal is designed for vehicular outdoor scenarios. On the other hand, Sionna is an open-source tool that allows for the inclusion of custom material properties, theoretically enabling its use at 300 GHz. It also offers a wide range of performance enhancements and comprehensive documentation. However, Sionna does not support time-variant or quasi-static scenario simulations, and it has not been tested at 300 GHz yet. Consequently, SiMoNe appears to be the most suitable tool for TIMES tasks. It has already been successfully employed for ray tracing at 300 GHz in indoor scenarios and has been calibrated using real measurements. SiMoNe offers the capability to simulate quasi-static scenarios and provides the opportunity to extend material properties libraries. It is important to note that SiMoNe is not publicly available but is being developed by TU Braunschweig, which is a project partner.

7.2 Overview of system-level simulation tools

In the following, we provide an overview of available system-level simulation tools, highlighting the main features and limitations related to the simulation of TIMES scenarios. Table 13 summarizes our findings.

SiMoNe system-level simulator

SiMoNe also integrates a system-level simulation tool for the performance evaluation of wireless systems [37]. Although the initial focus was the evaluation of Self Organizing Networks (SONs), the simulator has been extended over the years to include other scenarios, such as vehicular communications and wireless backhauling. This tool has been designed to work with real geographical data and realistic network topologies, enabling accurate network planning based on coverage and capacity needs. It supports multiple approaches for the modeling of signal propagation, including models for outdoor and indoor environments based on ray tracing and 3GPP-compliant models. Traffic demand and user distribution can be modeled at macroscopic and microscopic scales through traffic intensity maps or user-specific mobility models. Examples of studies that can be carried out with this tool include the analysis of cell load, investigation of radio link failures, and load balancing evaluation. Recently, SiMoNe was extended to support the modeling on wireless systems at THz frequencies. To this aim, ITU models to account for material parameters (ITU-R 2040-2 [40] atmospheric attenuation phenomena (ITU-R P.676-12 [51], ITU-R P.838-3 [52], ITU-R P.840-8 [53]) and field patterns of directional antennas (extension of ITU-R ITU-R F.1245-3 [54]) have been integrated. These functionalities were exploited to develop automatic planning algorithms for wireless backhauling at 300 GHz [55] and angle of arrival/departure estimation [56].

ns-3

ns-3 is a discrete-event simulator for networking systems released as open-source software and publicly maintained by a large community of developers. It has a modular design where each module accounts for the modelling of a different aspect of the system under investigation, such as user mobility, data traffic, signal propagation, communication protocols, etc. Each module provides one or multiple simulation models to describe the same phenomenon using different approaches or different levels of abstraction. ns-3 provides extensive support for the full-stack simulation of wireless systems. For example, the 5G-LENA and mmwave modules enable the simulation of cellular networks based on 3GPP 5G NR standards, while the wifi module supports the modeling of wireless LANs with multiple versions of the WiFi standard. It features 3GPP-compliant channel models for V2X and indoor factory scenarios, and it is possible to plug channel traces obtained from ray tracing simulations. In recent years, ns-3 was used to study the performance of THz systems. In [57], authors introduced an extension of THz communication networks which features dedicated models for PHY and MAC layers, as well as THz-specific channel and antenna models. It supports different application scenarios including nanoscale and macroscale networks.

Table 13 Overview of system level simulation tools

Tool	Type	Language	Open Source	Support to THz
SiMoNe system level simulator	Radio network level	C#	No	Yes
ns-3	Full-stack, end-to-end	C++	Yes	Yes, through TeraSim extension

In conclusion, both SiMoNe and ns-3 represent a good starting point for the system-level evaluation of protolcols, algorithms, and architectures developed within the context of this project. Some extensions may be required, for example to implement channel, mobility, and traffic models emulating specific scenarios and use cases.

7.3 Overview of link-level simulation tools

In this section, we present an overview of available link-level simulation tools for the performance evaluation of wireless links. A summary of our analysis is presented in Table 13.

Vienna Link Level Simulator

The Vienna 5G link-level simulation tool has been developed by University of Vienna [58]. This tool is implemented in Matlab and is accessible under an academic license. It offers a framework for conducting multi-node studies on orthogonal frequency division multiplexing (OFDM) based waveforms, channel coding, equalization schemes, as well as models for channel and antenna characteristics. Within this tool, the whole transmitter and receiver chain, as well as the wireless signal is implemented up to the individual signal samples, providing a very high level of accuracy. The simulator supports standard-compliant simulation of the physical downlink shared channel/physical uplink shared channel of LTE and 5G. However, due to object-oriented programming approach, it is possible to integrate some extra functionality: additional channel models [59], waveforms or modulation and coding schemes, to investigate candidate technologies of future mobile communication systems. The Vienna simulator also enables investigation, comparison, and optimization of flexible numerology for multicarrier waveforms, accommodating diverse service requirements and channel conditions, including delay and Doppler spread [60].
However, the spatial channel models used, which process time-discrete signals, are not specifically tailored to deterministic environments but rather operate at a more abstract level by incorporating stochastic functionalities. In the context of future links operating in the THz range, the performance of the system is highly influenced by the deployment environment. The Vienna 5G lacks the necessary functionalities to address these specific requirements [60].

HermesPy

HermesPy is an open-source tool designed for evaluating the physical layer performance of 6G wireless systems. Implemented in Python and C++ and distributed under the Affero General Public License. It follows an object-oriented, modular coding style. By default, HermesPy includes implementations for various communication waveforms like OFDM and single carrier (SC), as well as frequency-modulated continuous wave (FMCW), frequency shift keying (FSK) and along with state-of-the-art FEC codings, precodings, beamformers, and standard-compliant TDL and CDL channel models. Additionally, HermesPy offers the flexibility to configure MIMO coding and precoding at two specific stages within its communication signal processing chain: on the symbol level between mapping bits to data symbols and their modulation to base-

band signal representations, and on the antenna stream level after modulation and before transmission over the RF chain [61]. HermesPy is designed to support a wide range of carrier frequencies, that means that there is a possibility to use it for low THz communications simulation. However, (as far as authors are aware) there has been no research demonstrating the successful use of HermesPy for simulations in the low THz range.

Sionna link-level simulator

Sionna also integrates a link-level simulation tool that is written in Python and based on TensorFlow and Keras. All components are implemented as Keras layers, allowing the construction of sophisticated system architectures by connecting the desired layers in a similar manner to building a neural network. This tool includes 3GPP 38.901 Channel Models (TDL, CDL, RMa, UMa, Umi) and provides an AWGN model along with the capability to import channel impulse response (CIR) from datasets. Channel output computed in time or frequency domain. Sionna also has comprehensive documentation and wide range of tutorials. The weaknesses of this tool include the lack of multi-channel capability and the fact that Sionna doesn't include a system-level simulation tool [48] [62].

SiMoNe link-level simulator

Besides a system level simulator and a ray tracer, a SiMoNe also features a link-level simulator for THz communications. This simulator provides various single and multi-carrier waveforms [63] and among others, the modulations schemes of the IEEE Std 802.15.3d. For the THz communications the IEEE Std 802.15.3d foresees Reed Solomon and Low-Density Parity Check as channel coding, which are both available in SiMoNe. The channel impulse response found by the ray tracer of SiMoNe can be used to model the channel. Phase noise and the impairments of radio frequency devices on the signal are modeled, since the impact on the performance of the data transmission is crucial, especially for THz communications [64]. Part of the technical concept of SiMoNe is that the simulator is built on a modular composition. Functionalities are implemented in interchangeable and connectable modules. This allows to adapt the simulator to new concepts and ideas [64].

Table 14 Link-level simulation tools comparison

Tool	Language	Open source	Waveforms	Availability for THz	Real data transm.	Multi links	Included simulators
Vienna 5G	MATLAB	Yes	OFDM, Single Carrier	No	No	Yes	LL, SL
Sionna	Python	Yes	OFDM, Single Carrier	Yes	Yes	No	RT, LL
SiMoNe	C#	No	Single Carrier, Multi Carrier	Yes	Yes	Yes	RT, LL, SL
HermesPy	Python, C++	Yes	OFDM, Single Carrier	Yes	Yes	Yes	LL

All the link-level simulation tools presented above have some advantages, depending on the simulation target. In the context of the TIMES project, we need to work in the low THz range, making Vienna 5G unsuitable for our project tasks. Additionally, having the capability to work with multi-link simulations would be useful, so Sionna does not perfectly fit project requirements. Nevertheless, it can still be utilized for some project tasks, because of its good documentation and flexibility. Consequently, we are left to decide between

SiMoNe and HermesPy. On one hand, HermesPy is an open-source tool, while SiMoNe is closed source. On the other hand, HermesPy is solely a link-level simulator, whereas SiMoNe includes not only a link-level simulation tool but also system-level and RT simulators. Due to their integration within one framework, it is possible to execute propagation, link and system level simulations on the same simulation environment offering synergy effects for the investigations in industry scenarios.

8 Conclusions and Outlook

In this deliverable, we described models, parameters, and guidelines to be adopted for the software simulations within the context of this project. Different simulation methodologies have been considered, including ray tracing, link-level, and system-level simulation. In particular, we presented the digital models of two industrial environments to be used for the characterization of wireless propagation at THz frequencies. We described mobility models for industrial robots, and traffic models for different industrial applications. We proposed a list of parameters for the simulation of THz wireless terminals and presented a list of simulation scenarios based on TIMES' target use cases. Finally, we analyzed several simulation tools and identified the most suitable ones based on the projects' needs.

This deliverable should be used as a general reference to carry out software simulations in the context of this project. However, the ultimate decision on the specific tools, models, and parameters settings to be adopted is left to the partners, which can select them according to their needs. While this approach provides the opportunity to fulfil everyone's requirements, it might lead to inconsistent evaluations if the adopted configurations are not aligned across different partners. To mitigate this risk, we recommend partners working on the same task to agree on the specific settings to be used. The final choice will be documented in Deliverable 2.4.

9 References

[1] H. Niu, D. Dupleich, Y. Völker-Schöneberg, A. Ebert, R. Müller, J. Eichinger, A. Artemenko, G. D. Galdo and R. S. Thomä, "From 3D Point Cloud Data to Ray-tracing Multi-band Simulations in Industrial Scenario," in *2022 IEEE 95th Vehicular Technology Conference: (VTC2022-Spring)*, Helsinki, Finland, 2022.

[2] M. U. Sheikh, K. Ruttik, R. Jäntti and J. Hämäläinen, "Blockage and Ray Tracing Propagation Model in 3GPP Specified Industrial Environment," in *2021 International Conference on Information Networking (ICOIN)*, Jeju Island, Korea (South), 2021.

[3] S. Zhou et al., "Wireless Channel Simulation Platform for Industrial Environments Based on 3D Ray Tracing," in *2022 IEEE/CIC International Conference on Communications in China (ICCC)*, Sanshui, Foshan, China, 2022.

[4] M. Schmieder, T. Eichler, S. Wittig, M. Peter and W. Keusgen, "Measurement and Characterization of an Indoor Industrial Environment at 3.7 and 28 GHz," in *2020 14th European Conference on Antennas and Propagation (EuCAP)*, Copenhagen, Denmark, 2020.

[5] W. Hou, B. Du, Q. Wang, J. Du and X. Zhang, "Simulations and Analysis for Radio Wave Propagation Properties on 5G frequency Band in a Industrial Environment," in *2021 IEEE 5th Advanced Information Technology, Electronic and Automation Control Conference (IAEAC)*, Chongqing, China, 2021.

[6] Y. Wang, S. Safavi-Naeini and S. K. Chaudhuri, "A hybrid technique based on combining ray tracing and FDTD methods for site-specific modeling of indoor radio wave propagation," *IEEE Transactions on Antennas and Propagation,* May 2000.

[7] A. A. Agashe and S. Bodhe, "Performance Evaluation of Mobility Models for Wireless Ad hoc Networks," in *First International Conference on Emerging Trends in Engineering and Technology*, 2008.

[8] T. Camp, J. Boleng and V. Davies, "A survey of mobility models for ad hoc network research," *Wirel. Commun. Mob. Comput.,* 2002.

[9] L. D. Nardis and M. -G. D. Benedetto, "Mo3: A Modular Mobility Model for Future Generation Mobile Wireless Networks," *IEEE Access,* 2022.

[10] C. Sauer, E. Lyczkowski and M. Schmidt, "Mobility Models for the Industrial Peer-to-Peer Context Based on Empirical Investigation," in *2021 IEEE 32nd Annual International Symposium on Personal, Indoor and Mobile Radio Communications (PIMRC)*, Helsinki, Finland, 2021.

[11] M. D. Soltani, A. A. Purwita, H. H. Z. Zeng and M. Safari, "Modeling the Random Orientation of Mobile Devices: Measurement, Analysis and LiFi Use Case," *IEEE Transactions on Communications,* 2019.

[12] M. D. Soltani, A. A. Purwita, Z. Zeng, C. Chen, H. Haas and M. Safari, "An Orientation-Based Random Waypoint Model for User Mobility in Wireless Networks," in *2020 IEEE International Conference on Communications Workshops (ICC Workshops)*, Dublin, Ireland, 2020.

[13] 5G Alliance for Connected Industries and Automation, "A 5G Traffic Model," 2019.

[14] M. Gła¸bowski, S. Hanczewski, M. Stasiak, M. Weissenberg, P. Zwierzykowski and V. Bai, "Traffic Modeling in Industrial Ethernet Networks," *International Journal of Electronics and Telecommunications,* 2020.

[15] D. Kim, M. Ko, S. Kim, S. Moon, K. -Y. Cheon, S. Park, Y. Kim, H. Yoon and Y. -H. Choi, "Design and Implementation of Traffic Generation Model and Spectrum Requirement Calculator for Private 5G Network," *IEEE Access,* 2022.

[16] M. Lavassani, J. Åkerberg and M. Björkman, "Modeling and Profiling of Aggregated Industrial Network Traffic," *MDPI Journal of Applied Sciences,* 2022.

[17] TIMES, "Deliverable D2.1 - Definition of use cases, KPIs, and scenarios for channel measurements," 2023.

[18] Industrial Internet Consortium (IIC), "Time Sensitive Networks for Flexible Manufacturing Testbed - Description of Converged Traffic Types," 2018.

[19] T. Kürner et al., "Applications Requirement Document (ARD), DCN: 15-14-0304-16-003d, IEEE 802.15 TG3d," May 2015.

[20] Wireshark, 2023. [Online]. Available: https://www.wireshark.org/.

[21] U. R. Pfeiffer, R. Jain, J. Grzyb, S. Malz, P. Hillger and P. Rodriguez-Vizquez, "Current status of terahertz integrated circuits-from components to systems," in *IEEE BiCMOS and Compound Semiconductor Integrated Circuits and Technology Symposium (BCICTS)*, 2018.

[22] R. Han, Z. Hu, C. Wang, J. Holloway, X. Yi, M. Kim and J. Mawdsley, "Filling the gap: Silicon terahertz integrated circuits offer our best bet," *IEEE Microwave Magazine,* 2019.

[23] V. Petrov, T. Kurner and I. Hosako, "IEEE 802.15. 3d: First standardization efforts for sub-terahertz band communications toward 6G," *IEEE Communications Magazine,* 2020.

[24] I. Kallfass, F. Boes, T. Messinger, J. Antes, A. Inam, U. Lewark, A. Tessmann and R. Henneberger, "64 Gbit/s transmission over 850 m fixed wireless link at 240 GHz carrier frequency," *Journal of Infrared, millimeter, and terahertz waves,* 2015.

[25] A. A. Boulogeorgos, E. N. Papasotiriou and A. Alexiou, "Analytical performance assessment of THz wireless systems," *IEEE Access,* 2019.

[26] IEEE, "IEEE Standard for High Data Rate Wireless Multi-Media Networks–Amendment 2: 100 Gb/s Wireless Switched Point-to-Point Physical Layer," IEEE Std 802.15.3d-2017 (Amendment to IEEE Std 802.15.3- 2016 as amended by IEEE Std 802.15.3e-2017), 2017.

[27] P. Singh, B. W. Kim and S. Y. Jung, "TH-PPM with non-coherent detection for multiple access in electromagnetic wireless nanocommunications," *Nano Communication Networks,* 2018.

[28] A. Bemani, G. Cuozzo, N. Ksairi and M. Kountouris, "Affine frequency division multiplexing for next-generation wireless networks," in *2021 17th International Symposium on Wireless Communication Systems (ISWCS)*, 2021.

[29] L. Pucci, E. Paolini and A. Giorgetti, "System-level analysis of joint sensing and communication based on 5G new radio," *IEEE J. Sel. Areas Commun.,* 2022.

[30] L. H. Nguyen, V. Braun, H. Halbauer and T. Wild, "Waveform Comparison under Hardware Limitations for 6G Sub-THz Communications," in *IEEE 19th Annual Consumer Communications & Networking Conference (CCNC)*, Las Vegas, NV, USA, 2022.

[31] C. Buratti, G. Cuozzo and R. Verdone, "OCDMA: a MAC Protocol for Industrial Intra-machine TeraHertz Network," *Journal of Infrared, Millimeter and Terahertz Waves,* 2022.

[32] J. M. Eckhardt, A. Schultze, R. Askar, T. Doeker, M. Peter, W. Keusgen and T. Kürner, "Uniform Analysis of Multipath Components From Various Scenarios With Time-Domain Channel Sounding at 300GHz," *IEEE Open Journal of Antennas and Propagation,* 2023.

[33] C. Han, L. Yan and J. Yuan, "Hybrid beamforming for terahertz wireless communications: Challenges, architectures, and open problems," *IEEE Wireless Communications,* 2021.

[34] S. Bicais and J.-B. Dore, "Phase noise model selection for sub-THz communications," in *IEEE Global Communications Conference (GLOBECOM)*, 2019.

[35] X. Liu and H. C. Luong, "A Fully Integrated 0.27-THz Injection-Locked Frequency Synthesizer With Frequency-Tracking Loop in 65-nm CMOS," *IEEE Journal of Solid-State Circuits,* 2020.

[36] 3GPP, "TR 38.803, Radio Frequency (RF) and co-existence aspects (Release 14), v14.3.0," 2022.

[37] D. M. Rose, J. Baumgarten, S. Hahn and T. Kurner, "SiMoNe - Simulator for Mobile Networks: System-Level Simulations in the Context of Realistic Scenarios," in *2015 IEEE 81st Vehicular Technology Conference (VTC Spring)*, Glasgow, UK, 2015.

[38] TU Braunschweig, "SiMoNe - Simulator for Mobile Networks," [Online]. Available: https://www.tu-braunschweig.de/ifn/forschung/simone.

[39] F. Taleb, G. G. Hernandez-Cardoso, E. Castro-Camus and M. Koch, "Transmission, reflection and scattering characterisation of building materials for indoor THz communications," *IEEE Transactions on Terahertz Science and Technology,* 2023.

[40] ITU, "Effects of building materials and structures on radiowave propagation above about 100 MHz," Recommendation ITU-R P.2040-2, 2021 .

[41] J. M. Eckhardt, C. Herold, B. Friebel, N. Dreyer and T. Kürner, "Realistic Interference Simulations in a Data Center Offering Wireless Communication at Low Terahertz Frequencies," in *International Symposium on Antennas and Propagation (ISAP)*, Taipei, Taiwan, 2021 .

[42] E. Egea-Lopez, J. M. Molina-Garcia-Pardo, M. Lienard and P. Degauque, "Opal: An open source ray-tracing propagation simulator for electromagnetic characterization," *PLoS ONE,* 2021 .

[43] ITU, "Effects of building materials and structures," Recommendation ITU-R P.2040, 2013.

[44] E. Egea-Lopez, F. Losilla, J.Pascual-Garcia and J. M. Molina-Garcia-Pardo, "Vehicular Networks Simulation With Realistic Physics," *IEEE Access,* 2019 .

[45] Altair, “Altair WinProp datasheet,” 2023. [Online]. Available: hw_0000_datasheet_winprop_8.5x111011f42fb9e2442c843d89b0021ec11f.pdf.

[46] ITU, “Propagation data and prediction methods for the planning of short-range outdoor radiocommunication systems and radio local area networks in the frequency range 300 MHz to 100 GHz,” Recommendation P.1411-11, 2021.

[47] NVIDIA, “Sionna,” 2023. [Online]. Available: https://nvlabs.github.io/sionna/ .

[48] J. Hoydis, S. Cammerer, F. A. Aoudia, A. Vem, N. Binder, G. Marcus and A. Keller, “Sionna: An Open-Source Library for Next-Generation Physical Layer Research,” *arXiv preprint,* 2022.

[49] J. Hoydis, F. A. Aoudia, S. Cammerer, M. Nimier-Dsvid, N. Binder and G. Marcus, “Sionna RT: Differentiable Ray Tracing for Radio Propagation Modeling,” *arXiv preprint,* 2023.

[50] ITU, “Effects of building materials and structures on radiowave propagation above about 100 MHz,” Recommendation ITU-R P.2040-1, 2015.

[51] ITU-R P.676-12, “Attenuation by atmospheric gases and related effects,” August 2019.

[52] ITU-R P.838-3, “Specific attenuation model for rain for use in prediction methods,” March 2005.

[53] ITU-R P.840-8, “Attenuation due to clouds and fog,” August 2019.

[54] ITU-R F.1245-3, “Mathematical model of average and related radiation patterns for point-to-point fixed wireless system antennas for use in interference assessment in the frequency range from 1 GHz to 86 GHz,” January, 2019.

[55] B. K. Jung and T. K̈ürner, “Automatic Planning Algorithm of 300 GHz Backhaul Links Using Ring Topology,” in *15th European Conference on Antennas and Propagation (EuCAP)*, Dusseldorf, Germany, 2021.

[56] T. Doeker, P. R. Samala, P. S. Negi, A. Rajwade and T. Kürner, “Angle of Arrival and Angle of Departure Estimation Using Compressed Sensing for Terahertz Communications,” in *15th European Conference on Antennas and Propagation (EuCAP)*, Dusseldorf, Germany, 2021.

[57] Z. Hossain, Q. Xia and J. M. Jornet, “TeraSim: An ns-3 extension to simulate terahertz-band communication networks,” *Nano Communication Networks,* 2018.

[58] M. Rupp, S. Schwarz and M. Taranetz, The Vienna LTE-Advanced Simulators, Springer, 2016.

[59] A. Moller, J. Nuckelt, D. M. Rose and T. Kürner, “Physical Layer Performance Comparison of LTE and IEEE 802.11p for Vehicular Communication in an Urban NLOS Scenario,” in *IEEE 80th Vehicular Technology Conference (VTC2014-Fall)*, Vancouver, BC, Canada, 2014.

[60] S. Pratschner, B. Tahir, L. Marijanovic, M. Mussbah, K. Kirev, R. Nissel, S. Schwarz and M. Rupp, “Versatile mobile communications simulation: The Vienna 5G link level simulator,” *EURASIP Journal on Wireless Communications and Networking,* 2018.

[61] J. Adler, T. Kronauer and A. N. Barreto, “HermesPy: An Open-Source Link-Level Evaluator for 6G,” *IEEE Access,* 2022.

[62] NVIDIA, “Jumpstarting Link-Level Simulations with NVIDIA Sionna,” 2022. [Online]. Available: https://developer.nvidia.com/blog/jumpstarting-link-level-simulations-with-sionna/.

[63] J. M. Eckhardt, C. Herold and T. Kuerner, “Intercarrier Interference at Terahertz Frequencies for IEEE Std 802.15.3d Multiband Transmissions,” in *WSA & SCC 2023; 26th International ITG Workshop on Smart Antennas and 13th Conference on Systems, Communications, and Coding*, Braunschweig, Germany, 2023.

[64] J. M. Eckhardt, C. Herold, B. K. Jung, N. Dreyer and T. Kürner, “Modular link level simulator for the physical layer of beyond 5G wireless communication systems,” *Radio Sci.,* 2022.

[65] L. Samara, T. Zugno, M. Boban, M. Schellmann and T. Kürner, “Adapt and Aggregate: Adaptive OFDM Numerology and Carrier Aggregation for High Data Rate Terahertz Communications,” *IEEE Journal of Selected Topics in Signal Processing,* 2023.

[66] R. Zhang, K. Yang, Q. H. Abbasi, K. A. Qaraqe and A. Alomainy, “Analytical modelling of the effect of noise on the terahertz in-vivo communication channel for body-centric nano-networks,” *Nano communication networks,* 2018.

[67] X. Ouyang and J. Zhao, “Orthogonal chirp division multiplexing,” *IEEE Transactions on Communications,* 2016.